In Vivo Imaging of Foveal Sparing in Geographic Atrophy Secondary to Age-Related Macular Degeneration

Steffen Schmitz-Valckenberg, Monika Fleckenstein, Hans-Martin Helb, Peter Charbel Issa, Hendrik P. N. Scholl, and Frank G. Holz

Purpose. To investigate morphologic alterations in geographic atrophy caused by age-related macular degeneration (AMD) in the presence of foveal sparing using high-resolution in vivo imaging.

Methods. Simultaneous spectral domain optical coherence tomography (SD-OCT, 870 nm, 40,000 A-scans/s) and confocal scanning laser ophthalmoscopy (cSLO; fundus autofluorescence; excitation, 488 nm; emission, 500–700 nm) were performed in 18 eyes with geographic atrophy and foveal sparing using a combined instrument. Anatomic layers were evaluated, and retinal thickness in the fovea and the peripheral macula were measured and compared with those in controls of similar age.

Results. Fundus autofluorescence imaging showed an inhomogeneously reduced signal at the residual foveal island. SD-OCT scans disclosed mitigation of the foveal pit in the absence of extracellular fluid accumulation and an increased mean central retinal thickness of 248 ± 28 μm compared with 225 ± 12 μm in control eyes ($P = 0.005$). No difference in retinal thickness in the peripheral macula was observed (245 ± 16 vs. 253 ± 11 μm; $P = 0.6$). Subanalysis revealed marked appearance of swelling and widening of visible structures at the central outer nuclear layer (153 ± 22 μm vs. 127 ± 12 μm; $P = 0.003$). Below the external limiting membrane, a broad band of irregular high reflectivity was detected instead of the normal three separate reflective bands.

Conclusions. Thickening at the foveal site may reflect a preapoptotic stage of neuronal cellular elements indicating imminent atrophy. Limited structure-function correlation found in our study suggests that future therapeutic intervention may be beneficial in only a subset of AMD patients with foveal sparing. (*Invest Ophthalmol Vis Sci.* 2009;50:3915–3921) DOI:10.1167/iovs.08-2484

From the Department of Ophthalmology and Grade-Reading-Center, University of Bonn, Bonn, Germany.

Presented in part at the annual meeting of the Association for Research in Vision and Ophthalmology, Fort Lauderdale, Florida, May 2008.

Supported by German Research Council Grant Ho 1926/3-1 and by German Society of Ophthalmology Research Grant EU FP6.

Submitted for publication June 24, 2008; revised August 28 and December 17, 2008; accepted May 20, 2009.

Disclosure: **S. Schmitz-Valckenberg**, Heidelberg Engineering (F), Topcon UK (F); **M. Fleckenstein**, Heidelberg Engineering (F); **H.-M. Helb**, Heidelberg Engineering (F); **P. Charbel Issa**, Heidelberg Engineering (F); **H.P.N. Scholl**, Heidelberg Engineering (F); **F.G. Holz**, Heidelberg Engineering (C, F), Zeiss MediTec (C)

The publication costs of this article were defrayed in part by page charge payment. This article must therefore be marked "*advertisement*" in accordance with 18 U.S.C. §1734 solely to indicate this fact.

Corresponding author: Steffen Schmitz-Valckenberg, Department of Ophthalmology, University of Bonn, Ernst-Abbe-Strasse 2, 53127 Bonn, Germany; steffen.schmitz-valckenberg@ukb.uni-bonn.de.

Geographic atrophy (GA) represents the atrophic late-stage manifestation of dry age-related macular degeneration (AMD). It is responsible for approximately 35% of all cases with late AMD.[1,2] Despite the recent breakthrough by anti–vascular endothelial growth factor (VEGF) therapy for the active neovascular form, there is to date no proven treatment to prevent, halt, or slow down the GA disease process. Compared with neovascular AMD, GA tends to manifest in older patients; the incidence of GA has recently been found to be four times higher than for choroidal neovascularization in the population older than 85 years of age.[1] Given the increase in life expectancy and in AMD prevalence in general, it is expected that the absolute number and the proportion of patients with advanced atrophic AMD will increase in the future.

GA is characterized by the development of areas of outer retinal atrophy that slowly enlarge over time at a median rate of 1.5 to 2.1 mm^2 per year.[3–7] Atrophic areas of the retina are associated with a corresponding absolute scotoma (complete loss of retinal sensitivity). Therefore, atrophy enlargement is associated with progressive visual loss.[8,9] Typically, atrophic patches initially occur in the parafoveal retina. Over time, several atrophic areas may coalesce, and new atrophic areas may occur. This can result in a horseshoe configuration of atrophy. In advanced stages, atrophic areas may form a ring of the atrophy surrounding the fovea. On clinical examination, the fovea itself may remain uninvolved by the atrophic process until late in the course of the disease, a phenomenon referred to as foveal sparing.[10,11] When the fovea finally becomes involved, a dramatic loss in visual acuity occurs. After involvement of the central macula, little benefit can be expected from any future therapeutic intervention aiming to slow down or halt the natural course of the disease.[4,8] Overall, the exact pathophysiological mechanisms underlying the atrophic process, including the apparent relatively slower spread toward the fovea, are not yet understood. To identify rational therapeutic targets and to evaluate therapeutic interventions, we need a better understanding of the progression of GA.

The accumulation of lipofuscin in postmitotic human retinal pigment epithelial (RPE) cells and the adverse effects of its toxic compounds on normal cell function have been studied largely in vitro with fluorescence microscopic techniques.[12–17] Fundus autofluorescence (FAF) imaging with the confocal scanning laser ophthalmoscopy (cSLO) allows for visualization of the topographic distribution of lipofuscin over large retinal areas in vivo and, thus, for metabolic mapping of changes at the level of the retinal pigment epithelium.[18–22] In healthy subjects, retinal blood vessels (absorption by blood) and the optic nerve head (absence of the retinal pigment epithelium-related fluorophores) exhibit a very low FAF signal (Fig. 1).[23] The dip of the signal in the fovea is explained by the absorption of luteal pigment (lutein and zeaxanthin in the neurosensory retina). In addition, a higher melanin granule density and a lower density of lipofuscin granules in central RPE cells may represent additional contributory factors.[19] In patients with GA, FAF allows for accurate, noninvasive detection of atrophic

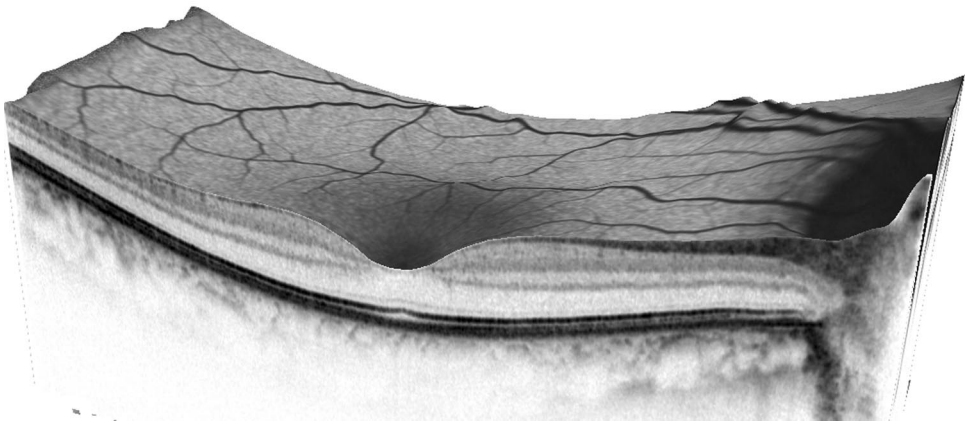

FIGURE 1. Spatial in vivo assessment with combined cSLO and SD-OCT of the foveal configuration and autofluorescence intensities in a healthy subject. Note the relatively decreased signal at the foveal dip, which was largely caused by the absorption of blue excitation light by luteal pigment.

patches that exhibit—because of the loss of retinal pigment epithelium and, therefore, fluorophores in lipofuscin granules—a markedly decreased signal. In retinal areas surrounding atrophy that show an increased signal, localized retinal sensitivity may be impaired.[9,24] Furthermore, we have shown, in the context of the prospective, multicenter natural history FAM (Fundus Autofluorescence in Age-Related Macular Degeneration) study, that abnormal patterns of increased FAF surrounding atrophy may serve as a prognostic marker for the future rate of progression of atrophy.[6,25] Not only do these observations underscore the pathophysiological role of excessive lipofuscin accumulation in GA, they demonstrate the clinical usefulness of FAF imaging with regard to monitoring patients with GA over time.

With the advent of spectral domain optical coherence tomography (SD-OCT), improved anteroposterior depth assessment for the in vivo visualization of microstructural alterations of the retina has become possible.[26,27] In particular, the combination of cSLO and SD-OCT in one instrument, together with real-time eye tracking, allows for accurate orientation of OCT scans and, therefore, for three-dimensional mapping of pathologic changes at specific anatomic sites.[28,29]

We have previously addressed high-resolution OCT findings in patients with GA in the perilesional, junctional, and actual atrophic zones.[28] In this study, with the use of high-resolution combined cSLO and SD-OCT in vivo imaging, we investigated morphologic alterations of the foveal retina at various anatomic layers in the presence of clinically visible foveal sparing in patients.

METHODS

Patients

Patients were recruited from the outpatient clinic at the Department of Ophthalmology, University of Bonn. The study followed the tenets of the Declaration of Helsinki. Informed consent was obtained from each patient after explanation of the nature and possible consequences of the study. Patients older than 50 years of age, with advanced atrophic AMD in at least one eye (unifocal or multifocal GA) and with a funduscopically visible residual foveal island, were enrolled. If both eyes met the inclusion criteria, both eyes were included. Exclusion criteria included any history of retinal surgery (including laser treatment), signs of diabetic retinopathy, history of retinal vascular occlusions, and any signs or history of hereditary retinal dystrophy. Fluorescein angiography was performed only if there were signs of neovascular AMD (extracellular fluid, hemorrhages, exudates, or fibrosis) in addition to well-delineated patches of GA. Such eyes were excluded from the study. Each patient underwent a routine ophthalmologic examination, including determination of best-corrected visual acuity using Snellen charts. Pupils were dilated with 1.0% tropicamide and 2.5% phenylephrine.

In Vivo Imaging

High-resolution in vivo imaging was carried out with a novel combined instrument (Spectralis HRA+OCT, Heidelberg Engineering, Heidelberg, Germany) that allows for simultaneous recording of cSLO and SD-OCT.[29] Initially, cSLO images were obtained according to a standardized operation protocol, which included the acquisition of near-infrared reflectance (λ = 830 nm) and FAF (λ = 480 nm, emission approximately 500–700 nm) images.[30] The size of the field of view encompassed 30° × 30° with an image resolution of 768 × 768 pixels. Subsequently, simultaneous SD-OCT scans were obtained using a second independent pair of scanning mirrors, as recently described.[28] Briefly, SD-OCT imaging is carried out with 870-nm illumination wavelength, an acquisition speed of 40,000 A-scans, and a scan depth of 1.8 mm. The digital depth resolution is approximately 3.5 μm/pixel. Live B-scans can be acquired and observed simultaneously in real-time to the cSLO image. Because of the two independent pairs of scanning mirrors, eye movements are registered and automatically corrected, allowing for pixel-to-pixel correlation of cSLO and OCT findings. With the high-speed mode used in this study, the transversal range of the B-scan thus encompasses 30° and consists of 768 A-scans. In the high-speed mode, the vertical presentation of the OCT scan is magnified twice (as with other OCT instruments); therefore, morphologic alterations are presented disproportionally high in the vertical dimension. In each study eye, vertical and horizontal OCT scans were obtained. To assess the foveal morphology, several horizontal OCT scans were placed through the center of the macula with a lateral inferior-superior distance between scans of at least 130 μm.

Fixation Testing

In a subset of patients, the locus, behavior, and stability of fixation were tested with automated fundus-correlated microperimetry (software version 1.5.1; MP1 Nidek Technologies, Padova, Italy) before in vivo imaging. Patients, whose pupils were dilated, were asked to fixate for 30 seconds on a 2° red fixation cross against a white background. The size of the cross was enlarged if the patient was not able to fixate. Data were recorded only while the eye tracking was active. Thus, no data were recorded during blinking or loss of tracking.

Image Analysis

For spatial assessment of the foveal structural changes, cSLO and SD-OCT scans were simultaneously studied side by side. The OCT scan nearest the foveal center was selected for each study eye. Retinal thickness measurements were carried out on these scans with the automated segmentation tool of the instrument (Heidelberg Eye Explorer; Heidelberg Engineering) in the presumed foveal center and at

approximately 3.5 mm temporally in the outer macula in the nonatrophic retina. At any given lateral position of the selected B-scan, retinal thickness is defined by the automated segmentation as the distance between the first signal from the vitreoretinal interface and the signal from the posterior boundary of the outermost high-reflective retinal band that presumably correlates with Bruch's membrane. Even this latter line was still subjectively visible; the automated segmentation failed to correctly define it in some eyes with marked drusen and deposition of material in the outer retina. In these cases, manual adjustment was performed. In a subanalysis and using the measurement tool of the software, the thickness of the first signal from the vitreoretinal interface to the outer part of the most inner hyperreflective band (presumably corresponding to the external limiting membrane) was manually assessed at the center of the fovea to quantify thickness changes in the outer nuclear layer. All thickness measurements were compared with 18 eyes of 18 control subjects of similar age (mean age, 70 years; range, 48–84). These normal eyes had no signs of AMD, such as drusen, or any other retinal abnormality as detected by stereo biomicroscopy and by cSLO and SD-OCT imaging.

Statistical Analysis

Statistical analyses included frequency and descriptive statistics. Retinal thickness measurements at the central fovea and at the peripheral macula were compared with 18 controls using the Wilcoxon signed ranks test. All statistical analyses were carried out with statistical software (SPSS 11.0; SPSS Inc., Chicago, IL).

Results

Eighteen eyes of 15 patients (mean age, 79.9 years; range, 68–99 years) were enrolled in the study. There were 11 women and 4 men. Bilateral GA was presented in nine patients, of whom three had foveal sparing in both eyes ($n = 6$ study eyes) and six had non-foveal sparing GA in the fellow eye ($n = 6$ study eyes). The other six study patients had unilateral GA with signs of exudative AMD in the fellow eye ($n = 6$ study eyes). One patient with bilateral GA (with foveal sparing in the study eye and non-foveal sparing GA in the fellow eye) had a documented history of bilateral anterior ischemic optic neuropathy with visual acuities of hand movements. Excluding this patient, median visual acuity was 20/50 (range, 20/125–20/25).

Instead of the symmetric annulus of decreased signal intensities present in healthy subjects, FAF imaging showed an irregularly reduced signal at the residual foveal island in all patients (Figs. 1, 2). SD-OCT scans revealed an overall increased retinal thickness with mitigation of the normal foveal pit. As described previously, the following bands can be disclosed below the hyporeflective band of the outer nuclear layer by SD-OCT at the fovea in healthy eyes: (1) a thin, hyperreflective band presumably corresponding to the external limiting membrane; (2) a slightly thicker hyperreflective band presumably corresponding to the interface of the inner and outer segments of the photoreceptor layer; (3) a thin, only occasionally visible, hyperreflective band presumably corresponding to the outer segment-retinal pigment epithelium interdigitation; and (4) a broad hyperreflective band thought to correspond to the retinal pigment epithelium/Bruch's membrane complex.[28,31] Compared with this normal configuration, an irregular and broad band of high reflectivity was seen in the study eyes at the site of the three outer hyperreflective bands (bands 2, 3, and 4); consequently, details were not longer visible. The external limiting membrane (band 1) was still detectable in all but four eyes. At the outer nuclear layer, SD-OCT imaging showed the marked appearance of swelling and widening of visible structures. Next to the foveal center, the inner retinal layers disclosed, in the presence of foveal sparing, a convex shape rather than the normal concave configuration. The inner retinal layers appeared to be distorted and to have a tendency toward perifoveal atrophy. At the site of atrophy, marked retinal thinning and absence of the characteristic morphology of outer retinal layers were present.

Automated segmentation revealed a mean retinal thickness in the central fovea of 248 ± 28 μm (range, 206–318) compared with 225 ± 12 μm (range, 200–251) in controls (Figs. 3, 4). This difference was statistically significant ($P = 0.005$; Wilcoxon signed ranks test). By contrast, no significant difference was found at the peripheral macula, with a mean retinal thickness of 245 ± 16 μm (range, 221–279) for patients with AMD and 253 ± 11 μm (range, 237–276) for controls ($P = 0.4$). To determine which retinal layers primarily contributed to the overall increased thickness, we performed additional measurements above (inner portion, including the external

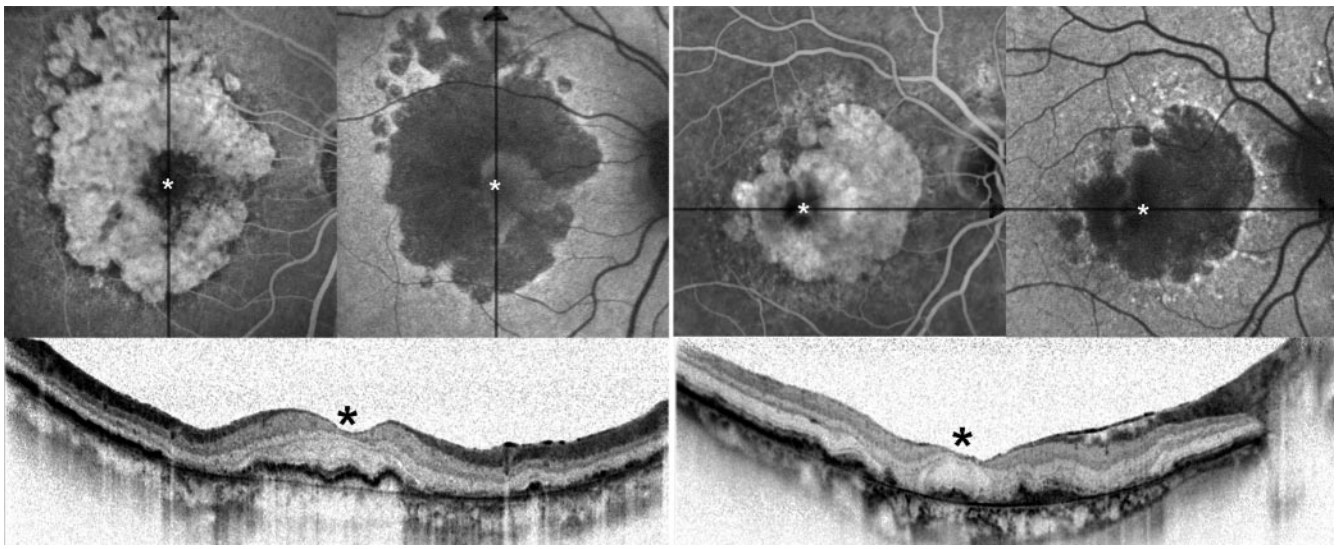

Figure 2. Two examples with late-phase fluorescein angiography, fundus autofluorescence, and SD-OCT of patients with geographic atrophy secondary to AMD and clinically visible foveal sparing. The *black lines* through the fovea on the fundus images correlate to the location of the tomographic SD-OCT scans; the *asterisk* represents the center of the fovea. Note the irregular distribution of relatively decreased autofluorescence and the mitigation of the foveal pit with marked changes in reflectivity at different layers by SD-OCT imaging at the residual island.

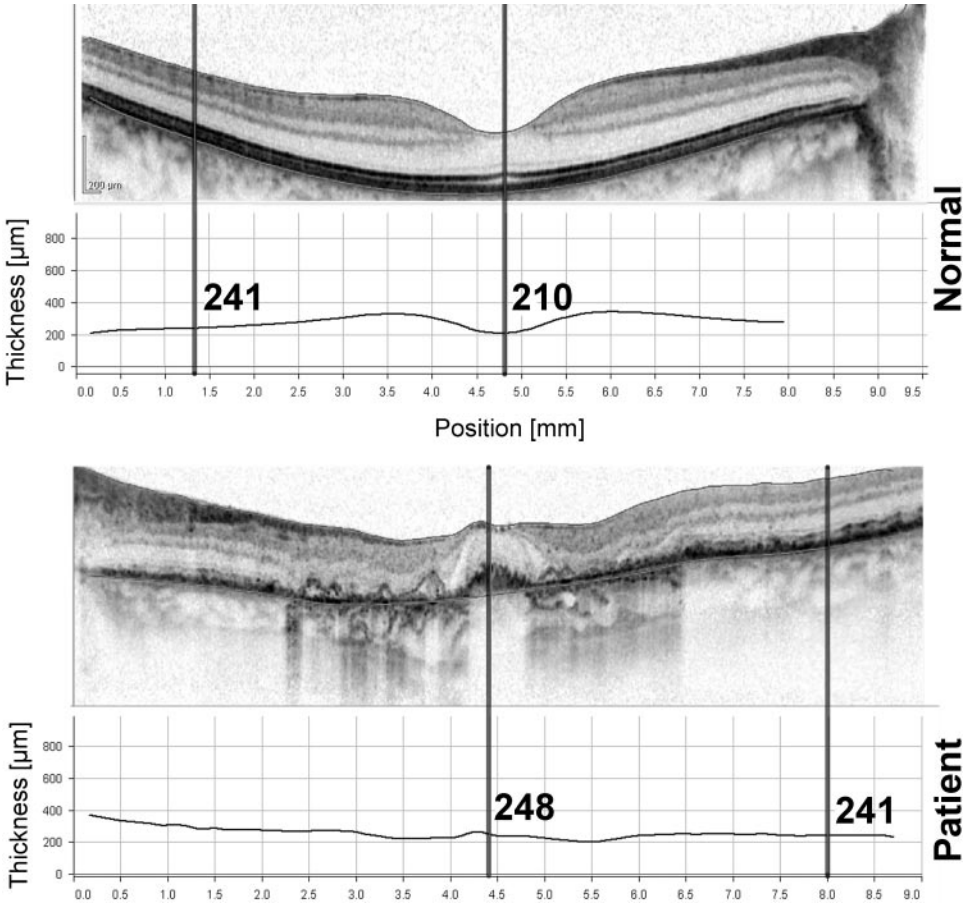

FIGURE 3. Illustration of analysis strategy for thickness measurements on SD-OCT scans, shown in a healthy subject (*top*) and in a patient with age-related geographic atrophy and clinically visible foveal sparing (*bottom*). The first signal from the vitreoretinal interface and the signal from the posterior boundary of the outermost high-reflective retinal band (presumably Bruch's membrane) are outlined by automated segmentation. This allows for retinal thickness measurements at the foveal center and approximately 3.5 mm temporally in the peripheral (nonatrophic) macula. Note the difference in retinal thickness between the foveas of a healthy subject (210 μm) and a patient (248 μm); no change is found in the peripheral macula (each 241 μm).

limiting membrane) and below (outer portion) the presumed external limiting membrane, where this line was delineable. For the inner portion, thickness was 153 $\pm$ 22 μm (range, 119–190) for patients with AMD and 127 $\pm$ 12 μm (range, 102–148) for controls, respectively ($P = 0.003$). By contrast, no significant changes were noted for the retinal thickness of the outer portion ($P = 0.8$).

Location and stability of fixation were documented using the automated fundus-correlated microperimeter (MP1 Nidek Technologies) in seven representative eyes (Fig. 5). All but two showed stable fixation at the residual foveal island with fixation within 2° from the center of the target during 86% to 100% of the test time. By contrast, two eyes each were found to have an eccentric preferred retinal locus (PRL) at the edge of the central atrophy. Fixation was rated as relatively instable, with 43% and 71% of test time within 2° from this locus. Both eyes had clinical visible foveal sparing, marked irregular FAF intensities in the central macula, and typical SD-OCT findings with thickening and disappearance of the foveal pit, as described. Visual acuities were 20/50 and 20/80. When asked, patients were able to spot a target in the center over the residual island but obviously used an eccentric PRL for other tasks. Indeed,

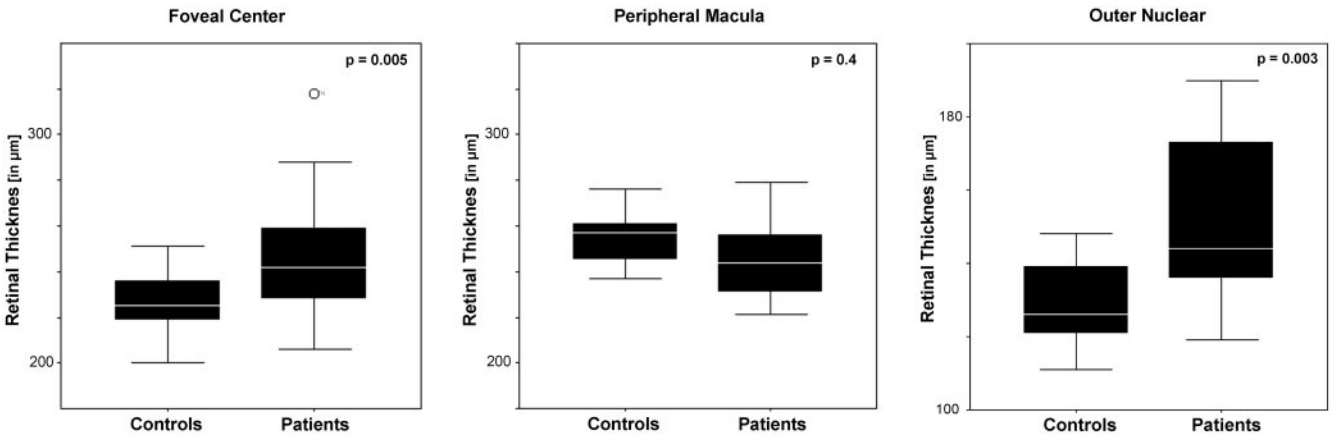

FIGURE 4. Box plots for retinal thickness measurements. Note the statistical difference for the foveal center ($P = 0.005$) between controls and patients; only minor changes are found for the peripheral macula. Subanalysis revealed that the increased thickness was located at the outer nuclear layer.

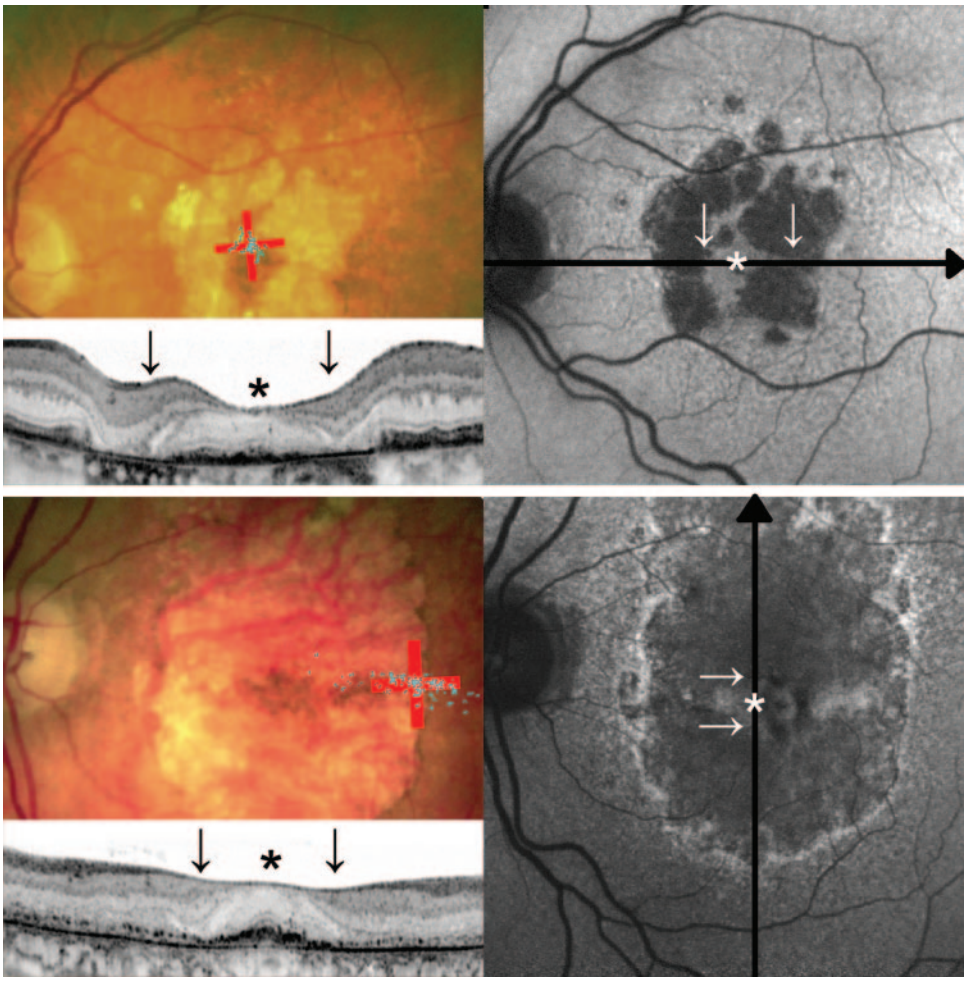

FIGURE 5. Two examples for clinical visible foveal sparing in patients with age-related geographic atrophy with testing results of the preferred retinal fixation locus, cSLO autofluorescence imaging and SD-OCT scans through the fovea (scans are magnified for illustration and encompass only approximately the central retina). Although fixation is located at the fovea (*top*), the patient has an eccentric preferred retinal locus of fixation at the edge of atrophy (*bottom*). For the latter, visual acuity was 20/50. During the examination, fixation occasionally switched toward the central funduscopically nonatrophic retina but rapidly returned to the eccentric site. The *black lines* through the fovea on the autofluorescence images correlate to the location of the tomographic SD-OCT scan, and the *asterisk* represents the center of the fovea. The *arrows* mark the beginning of atrophy next to the foveally spared island according to the pixel-to-pixel correlation of the combined cSLO and SD-OCT instrument.

during the examination, these patients occasionally fixated within the clinical visible area of foveal sparing but rapidly switched back to the eccentric PRL.

DISCUSSION

This study demonstrates that in vivo examination by novel combined cSLO and SD-OCT imaging techniques in patients with GA reveals complex microstructural alterations in the central retina in the presence of advanced, surrounding atrophy. Performed separately, cSLO and OCT imaging offered new insights into retinal diseases in the past. This study indicates that the simultaneous application of both techniques and the use of the eminent advantages of each imaging modality in combination may add to our understanding of retinal disorders and their pathologic mechanisms.

The phenomenon of foveal sparing despite progressive spread of atrophy is well known in GA and has attracted particular attention.[8,10,32–36] In patients with foveal sparing, Sunness et al.[8] have reported that measurement of central visual acuity hardly reflects the actual visual function of the patient, such as reading speed, and that central visual acuity correlates poorly with total GA size at this stage. Furthermore, a typical clinical observation is that a patient may be able to spot a single letter on the test chart and have a good central visual acuity score but may be unable to read larger words or to recognize faces. By investigating the behavior of fixation with fundus-controlled testing, we could confirm that some patients were able to spot the fixation cross at the residual foveal island, though their PRL was already displaced at the edge of atrophy. In the past, authors have explained these observations by the small size of the residual foveal island and the resultant limited extent of the central visual field.[32] A full face or words would, therefore, not fit in the spared fovea surrounded by atrophy. However, until today, structural changes in the presence of foveal sparing have not been investigated because of the lack of adequate imaging technologies. The structural alterations observed in this study suggest that the reduced foveal function and the selection of an eccentric PRL in some patients may not be just a matter of the size of the residual island. Even if some function of the fovea is left, the marked morphologic involvement of cell layers may already cause severe dysfunction. On the contrary, we observed limited structure-function correlation in other patients. A subset of patients exhibited preserved fixation and central visual acuity in presence of marked morphologic alterations.

The widening of visible structures at the outer nuclear layer noted herein may represent a morphologic correlate of an early apoptotic stage. Incipient photoreceptor apoptosis in postmortem studies is morphologically characterized by extension of the cellular volume and disintegration of nuclei.[37] This would be in line with the increased retinal thickness in the outer nuclear layer seen in this study in the absence of extracellular fluid accumulation. Furthermore, it might be conceivable that the increased reflectivity at the outer retina may relate to the development of incipient atrophy, though the precise substrate for this reflectivity change is unknown. Because bands 2, 3, and 4 were not delineable, it was not possible to disclose to

which extent layers above Bruch's membrane were affected and to reveal the exact anteroposterior location of the hyperreflective material. Another explanation for the extension and thickening of the outer nuclear layer might be mechanical stress. It is conceivable that the normal configuration of photoreceptors is partially loosened by the disappearance of outer retinal material around the foveal center. Hereby, photoreceptor segments might be torn away toward eccentricity leading to widening of their nuclei

The reason for the relatively slower spread of atrophy toward the foveal center remains unclear. Several authors have considered a preferential vulnerability of the rod system and relative stability of the cone system in AMD. This hypothesis is underscored by histologic and clinical data.[24,38–43] Scotopic sensitivity loss is more severely affected than photopic sensitivity over areas with increased FAF.[24] Furthermore, retinal function of patients with GA decreases greatly under dim light conditions, and high luminance levels are required for reading.[35] Another well-documented observation is that visual loss is usually perceived by the patient as gradual, even when considerable decreases in visual acuity occur and when foveal vision and fixation are lost.[10] This perception has been explained by a possible transitional period during which a patient uses foveal and extrafoveal site for fixation. It may be hypothesized that cones and rods are both affected by severe functional impairment of the underlying corresponding retinal pigment epithelium related to Bruch's membrane and choriocapillaris alterations. The time interval from early involvement and dysfunction to cell death may be longer for cones than for rods. This hypothesis, which is underscored by the structural changes revealed in this study, would help to explain not only the clinically apparent slow GA spread toward the fovea and the slow involvement of foveal areas in atrophy but also the relative foveal cone dysfunction in the presence of clinical visible foveal sparing.

Foveal preservation has been regarded as a promising target for future therapies. The results of this study suggest that loss of the normal foveal configuration and distinct morphologic changes within the foveal retina may already occur in what clinically appears to be foveal sparing. If a programmed cascade of foveal cell death is already in action at this stage, intervention would have to be administered at earlier disease stages to rescue foveal photoreceptors. In this case, the spatial assessment of the central macula with combined SD-SLO imaging technology may be helpful to select patients who may be more likely to benefit from a future treatment. Furthermore, the structural alterations may serve as a clinical marker for the response to treatment, such as if remodeling is achieved with normalization of the foveal contour.

One limitation of the study is the cross-sectional analysis and the lack of longitudinal observations. Therefore, we cannot exclude that foveal changes, such as thickness or alterations in the OCT signal, occurred before the development of foveal sparing of atrophy. However, until now, we had not seen any of the typical changes described in patients with extrafoveal GA patches of lesser extent. We did not perform fluorescein angiography in all study patients. This was performed only if any sign for corneal neovascularization was noted. Therefore, we cannot exclude that some patients could have had neovascularization before atrophy developed. However, all patients had the appearance of pure GA by stereo biomicroscopy. In addition, there were no signs of fibrosis or sub-RPE material by cSLO and OCT imaging as they are commonly encountered in patients with disciform scars.

In summary, this study reveals previously unknown distinct structural foveal alterations by using combined high-resolution cSLO and OCT imaging in patients with GA clinically sparing the foveal retina. Notably, the loss of the normal foveal configuration occurred despite relatively preserved central visual acuity and in the absence of any cystoid spaces. These findings may suggest an already pre-apoptotic stage of foveal neuronal cellular elements and the development of incipient atrophy before cell death. This may be important for therapeutic interventions aiming to slow the progression of atrophy. Longitudinal observations correlating function and morphology are warranted to better understand the dynamic process and evolution of foveal atrophy in patients with GA caused by AMD.

Acknowledgments

The authors thank Boris Airo and Gero Tietz for their enduring efforts in imaging patients, and Maria Hofmann and Kerstin Bartsch for their outstanding support.

References

1. Klein R, Klein BE, Knudtson MD, Meuer SM, Swift M, Gangnon RE. Fifteen-year cumulative incidence of age-related macular degeneration: the Beaver Dam Eye Study. *Ophthalmology.* 2007; 114:253–262.
2. Augood CA, Vingerling JR, de Jong PT, et al. Prevalence of age-related maculopathy in older Europeans: the European Eye Study (EUREYE). *Arch Ophthalmol.* 2006;124:529–535.
3. Sunness JS. The natural history of geographic atrophy, the advanced atrophic form of age-related macular degeneration. *Mol Vis.* 1999;5:25.
4. Maguire P, Vine AK. Geographic atrophy of the retinal pigment epithelium. *Am J Ophthalmol.* 1986;102:621–625.
5. Schatz H, McDonald HR. Atrophic macular degeneration: rate of spread of geographic atrophy and visual loss. *Ophthalmology.* 1989;96:1541–1551.
6. Holz FG, Bindewald-Wittich A, Fleckenstein M, et al. Progression of geographic atrophy and impact of fundus autofluorescence patterns in age-related macular degeneration. *Am J Ophthalmol* 2007; 143:463–472.
7. Sunness J, Margalit E, Srikurnaran D, et al. The long-term natural history of geographic atrophy from age-related macular degeneration. *Ophthalmology.* 2007;114:271–277.
8. Sunness JS, Gonzalez-Baron J, Applegate CA, et al. Enlargement of atrophy and visual acuity loss in the geographic atrophy form of age-related macular degeneration. *Ophthalmology.* 1999;106: 1768–1779.
9. Schmitz-Valckenberg S, Bultmann S, Dreyhaupt J, Bindewald A, Holz FG, Rohrschneider K. Fundus autofluorescence and fundus perimetry in the junctional zone of geographic atrophy in patients with age-related macular degeneration. *Invest Ophthalmol Vis Sci.* 2004;45:4470–4476.
10. Sunness JS, Bressler NM, Maguire MG. Scanning laser ophthalmoscopic analysis of the pattern of visual loss in age-related geographic atrophy of the macula. *Am J Ophthalmol.* 1995;119:143–151.
11. Sarks JP, Sarks SH, Killingsworth MC. Evolution of geographic atrophy of the retinal pigment epithelium. *Eye.* 1988;2 552–577.
12. Bergmann M, Schutt F, Holz FG, Kopitz J. Inhibition of the ATP-driven proton pump in RPE lysosomes by the major lipofuscin fluorophore A2-E may contribute to the pathogenesis of age-related macular degeneration. *FASEB J.* 2004;18:562–564.
13. Boulton M, Dayhaw-Barker P. The role of the retinal pigment epithelium: topographical variation and ageing changes. *Eye.* 2001;15:384–389.
14. Feeney-Burns L, Berman ER, Rothmann H. Lipofuscin of human retinal pigment epithelium. *Am J Ophthalmol.* 1980;90:783–791.
15. Katz ML. Potential role of retinal pigment epithelial lipofuscin accumulation in age-related macular degeneration. *Arch Gerontol Geriatr.* 2002;34:359–370.
16. Katz ML, Robison WG Jr. What is lipofuscin? Defining characteristics and differentiation from other autofluorescent lysosomal storage bodies. *Arch Gerontol Geriatr.* 2002;34:169–184.
17. Sparrow JR, Boulton M. RPE lipofuscin and its role in retinal pathobiology. *Exp Eye Res.* 2005;80:595–606.

18. von Ruckmann A, Fitzke FW, Bird AC. Distribution of fundus autofluorescence with a scanning laser ophthalmoscope. *Br J Ophthalmol.* 1995;79:407–412.
19. Delori FC, Dorey CK, Staurenghi G, Arend O, Goger DG, Weiter JJ. In vivo fluorescence of the ocular fundus exhibits retinal pigment epithelium lipofuscin characteristics. *Invest Ophthalmol Vis Sci.* 1995;36:718–729.
20. Bellmann C, Holz FG, Schapp O, Volcker HE, Otto TP. [Topography of fundus autofluorescence with a new confocal scanning laser ophthalmoscope]. *Ophthalmologe.* 1997;94:385–391.
21. Schmitz-Valckenberg S, Holz FG, Bird AC, Spaide RF. Fundus autofluorescence imaging: review and perspectives. *Retina.* 2008;28:385–409.
22. Schmitz-Valckenberg S, Fleckenstein M, Scholl HP, Holz FG. Fundus autofluorescence and progression of age-related macular degeneration. *Surv Ophthalmol.* 2009;54:96–117.
23. Holz FG, Schmitz-Valckenberg S, Spaide RF, Bird AC. *Atlas of Fundus Autofluorescence Imaging.* Berlin: Springer; 2007.
24. Scholl HP, Bellmann C, Dandekar SS, Bird AC, Fitzke FW. Photopic and scotopic fine matrix mapping of retinal areas of increased fundus autofluorescence in patients with age-related maculopathy. *Invest Ophthalmol Vis Sci.* 2004;45:574–583.
25. Schmitz-Valckenberg S, Bindewald-Wittich A, Dolar-Szczasny J, et al. Correlation between the area of increased autofluorescence surrounding geographic atrophy and disease progression in patients with AMD. *Invest Ophthalmol Vis Sci.* 2006;47:2648–2654.
26. Drexler W, Morgner U, Ghanta RK, Kartner FX, Schuman JS, Fujimoto JG. Ultrahigh-resolution ophthalmic optical coherence tomography. *Nat Med.* 2001;7:502–507.
27. Wojtkowski M, Bajraszewski T, Gorczynska I, et al. Ophthalmic imaging by spectral optical coherence tomography. *Am J Ophthalmol.* 2004;138:412–419.
28. Fleckenstein M, Charbel Issa P, Helb HM, et al. High-resolution spectral domain-OCT imaging in geographic atrophy associated with age-related macular degeneration. *Invest Ophthalmol Vis Sci.* 2008;49:4137–4144.
29. Helb HM, Charbel Issa P, Fleckenstein M, et al. Clinical evaluation of simultaneous confocal scanning laser ophthalmoscopy imaging combined with high-resolution, spectral-domain optical coherence tomography. *Ophthalmologica.* In press.
30. Schmitz-Valckenberg S, Fleckenstein M, Gobel AP, et al. Evaluation of autofluorescence imaging with the scanning laser ophthalmoscope and the fundus camera in age-related geographic atrophy. *Am J Ophthalmol.* 2008;146:183–192.
31. Srinivasan VJ, Monson BK, Wojtkowski M, et al. Characterization of outer retinal morphology with high-speed, ultrahigh-resolution optical coherence tomography. *Invest Ophthalmol Vis Sci.* 2008;49:1571–1579.
32. Sunness JS, Applegate CA, Haselwood D, Rubin GS. Fixation patterns and reading rates in eyes with central scotomas from advanced atrophic age-related macular degeneration and Stargardt disease. *Ophthalmology.* 1996;103:1458–1466.
33. Sunness JS, Massof RW, Johnson MA, Bressler NM, Bressler SB, Fine SL. Diminished foveal sensitivity may predict the development of advanced age-related macular degeneration. *Ophthalmology.* 1989;96:375–381.
34. Sunness JS, Rubin GS, Applegate CA, et al. Visual function abnormalities and prognosis in eyes with age-related geographic atrophy of the macula and good visual acuity. *Ophthalmology.* 1997;104:1677–1691.
35. Sunness JS, Rubin GS, Broman A, Applegate CA, Bressler NM, Hawkins BS. Low luminance visual dysfunction as a predictor of subsequent visual acuity loss resulting from geographic atrophy in age-related macular degeneration. *Ophthalmology.* 2008;115:1480–1488.
36. Sunness JS, Schuchard RA, Shen N, Rubin GS, Dagnelie G, Haselwood DM. Landmark-driven fundus perimetry using the scanning laser ophthalmoscope. *Invest Ophthalmol Vis Sci.* 1995;36:1863–1874.
37. Wenzel A, Grimm C, Samardzija M, Reme CE. Molecular mechanisms of light-induced photoreceptor apoptosis and neuroprotection for retinal degeneration. *Prog Retin Eye Res.* 2005;24:275–306.
38. Chen C, Wu L, Wu D, et al. The local cone and rod system function in early age-related macular degeneration. *Doc Ophthalmol.* 2004;109:1–8.
39. Curcio CA. Photoreceptor topography in ageing and age-related maculopathy. *Eye.* 2001;15:376–383.
40. Curcio CA, Millican CL, Allen KA, Kalina RE. Aging of the human photoreceptor mosaic: evidence for selective vulnerability of rods in central retina. *Invest Ophthalmol Vis Sci.* 1993;34:3278–3296.
41. Jackson GR, Owsley C, Curcio CA. Photoreceptor degeneration and dysfunction in aging and age-related maculopathy. *Ageing Res Rev.* 2002;1:381–396.
42. Owsley C, Jackson GR, Cideciyan AV, et al. Psychophysical evidence for rod vulnerability in age-related macular degeneration. *Invest Ophthalmol Vis Sci.* 2000;41:267–273.
43. Chuang EL, Sharp DM, Fitzke FW, Kemp CM, Holden AL, Bird AC. Retinal dysfunction in central serous retinopathy. *Eye.* 1987;1(pt 1):120–125.